HHS Public Access

Author manuscript

Nat Med. Author manuscript; available in PMC 2012 April 23.

Published in final edited form as:

Nat Med. ; 17(11): 1490–1497. doi:10.1038/nm.2461.

Tissue factor-PAR2 signaling promotes diet-induced obesity and adipose inflammation

Leylla Badeanlou[1], **Christian Furlan-Freguia**[2], **Guang Yang**[1], **Wolfram Ruf**[2,3], and **Fahumiya Samad**[1,3]

[1]Department of Cell Biology, Torrey Pines Institute for Molecular Studies, San Diego, CA, USA

[2]Department of Immunology and Microbial Science, The Scripps Research Institute, La Jolla, CA, USA

Abstract

Tissue factor (TF), the initiator of the coagulation cascade, mediates coagulation factor VIIa-dependent activation of protease activated receptor-2 (PAR2). Here we delineate an unexpected role for coagulation signaling in obesity and its complications. Mice lacking PAR2 (*F2rl1*) or the cytoplasmic domain of TF (*F3*) are protected from high fat diet (HFD) induced weight gain and insulin resistance. In hematopoietic cells, genetic deletion of TF-PAR2 signaling reduces adipose tissue macrophage inflammation and specific pharmacological inhibition of macrophage TF signaling rapidly ameliorates insulin resistance. In contrast, non-hematopoietic cell TF-VIIa-PAR2 signaling specifically promotes obesity. Mechanistically, adipocyte TF cytoplasmic domain dependent VIIa signaling suppresses Akt phosphorylation with concordant adverse transcriptional changes of key regulators of obesity and metabolism. Pharmacological blockade of adipocyte TF in vivo reverses these effects of TF-VIIa signaling and rapidly improves energy expenditure. Thus, TF signaling is a potential therapeutic target to improve impaired metabolism and insulin resistance in obesity.

G-protein-coupled receptor (GPCR) signaling regulates obesity[1] and modulates adipose tissue macrophage-dependent inflammation[2]. While crucial regulators of adipose tissue macrophages have been identified[2–6], extracellular signals sustaining their proinflammatory phenotype in obesity are unclear. The adaptor protein β-arrestin 2 terminates as well as mediates signaling of certain GPCRs[7, 8] and is important in insulin signaling[9]. The GPCR protease activated receptor 2 (PAR2), signals through G protein activation and recruits β-arrestins for scaffolding of cytoskeletal regulators as well as for suppression of phosphatidyl

---

[3]Correspondence to Wolfram Ruf, ruf@scripps.edu and Fahumiya Samad, fsamad@tpims.org.

Author contributions

L.B. and C.F.F. made equally significant contributions to these studies and share the first authorship. L.B. performed metabolic, gene expression, and in vitro experiments and analyzed data, C.F.F. generated BM chimeras, performed FACS analysis and analyzed data. G.Y. performed the *in vivo* and *in vitro* Akt activation assays. W.R. and F.S. designed experiments, analyzed data and wrote the manuscript and share the last authorship.

Competing Financial Interests

W. Ruf and F. Samad have pending patent applications on the use of anti-TF antibodies to ameliorate obesity and insulin resistance.

inositol 3 kinase (PI3K) dependent Akt phosphorylation[8, 10, 11]. In adipocytes, β-arrestin 2 suppresses adenosine monophosphate-activated protein kinase (AMPK) activation induced by PAR2 G protein-coupled signaling[12], but it remained unexplored whether PAR2 can influence diet-induced obesity (DIO).

Obesity induces prothrombotic molecules (plasminogen activator inhibor-1[PAI-1], tissue factor [TF]) that are implicated in metabolic and cardiovascular complications[13, 14] attributed to elevated circulating TF[15–17]. However, functional roles of increased TF in adipose tissues of obese mice[18] are unknown. A range of serine proteases activate PAR2, but coagulation factor VIIa in complex with TF uniquely regulates cell migration though PAR2 activation and phosphorylation-dependent crosstalk of the TF cytoplasmic domain with integrins[19]. TF-PAR2 signaling also promotes cancer progression and myeloid cell inflammatory signaling leading to fetal loss syndrome[20, 21] and mice lacking the TF cytoplasmic domain ($TF^{\Delta CT}$ mice) phenocopy PAR2-deficiency, demonstrating required contributions of the TF cytoplasmic domain in pathological TF-PAR2 signaling. The cellular pool of TF involved in cell signaling is recognized by a specific anti-human TF antibody (10H10)[22] that blocks TF-VIIa-PAR2 signaling[21, 23] without inhibiting downstream coagulation signaling. Here, we made use of these novel genetic and pharmacological tools to uncover an unexpected signaling pathway in obesity. We delineate that TF-VIIa-PAR2 signaling of adipocytes is a crucial regulator of weight gain, while independently TF-PAR2 signaling of adipose tissue macrophages promotes inflammation leading to insulin resistance.

Results

TF cytoplasmic domain or PAR2 deficiency attenuate DIO

TF activity in plasma and in epididymal visceral adipose tissue (VAD) extracts was upregulated in mice on a HFD for 16 weeks (Fig. 1a) concordant with elevations of VAD mRNA of TF and its signaling receptor PAR2 (Fig. 1b). Body weights of aged, syngeneic C57BL/6 male mice on a normal low fat chow diet (Supplementary Fig. 1a) indicated that TF cytoplasmic domain and PAR2 signaling, but not the thrombin receptor PAR1 contribute to body weight regulation by the TF pathway. On a HFD, WT mice gained weight rapidly, whereas weight gain was reduced in $TF^{\Delta CT}$ or *F2rl1*$^{-/-}$ mice. $TF^{\Delta CT}$/*F2rl1*$^{-/-}$ mice showed no additive effects (Fig.1c) and both mutations caused significantly reduced fat pad weights (Supplementary Fig. 1b), indicating that the mutations protect from DIO by a similar mechanism.

HFD $TF^{\Delta CT}$ mice had reduced plasma levels of free fatty acids (FFA), fasting insulin, glucose, and showed improved glucose homeostasis in insulin and glucose tolerance tests (Fig. 1d; Supplementary Fig. 2a, b). Pronounced insulin-induced phosphorylation of Akt in adipose tissue confirmed improved insulin sensitivity of HFD $TF^{\Delta CT}$ mice in comparison to non-responsive WT controls (Fig. 1d). Similarly, *F2rl1*$^{-/-}$ and $TF^{\Delta CT}$/*F2rl1*$^{-/-}$ mice had lower plasma FFA, fasting insulin and glucose levels, and improved glucose homeostasis relative to WT (Fig 1e; Supplementary Fig. 2c, d). Thus, loss of the TF cytoplasmic domain or PAR2 signaling produced a similar and non-additive improvement in obesity and insulin resistance.

Chronic inflammation specifically in VAD is linked to proinflammatory adipose tissue F4/80$^+$/CD11b$^+$/CD11c$^+$ macrophages/dendritic cells[24]. Depletion of CD11c$^+$ cells shifts the balance to M2 polarized F4/80$^+$/CD11b$^+$/CD11c$^-$ macrophages expressing high levels of the anti-inflammatory cytokine IL-10 and improves insulin sensitivity[25]. CD11b$^+$/CD11c$^+$ pro-inflammatory macrophages aggregate around apoptotic adipocytes to form "crown like structures" (CLS)[26]. CLS were reduced in TF$^{\Delta CT}$ and *F2rl1*$^{-/-}$ mice (Fig. 1f). FACS analysis of adipose stromal vascular fraction (SVF) cells of HFD WT, TF$^{\Delta CT}$, *F2rl1*$^{-/-}$ and TF$^{\Delta CT}$/*F2rl1*$^{-/-}$ mice showed that obesity-protected strains had reduced numbers of CD11b$^+$/CD11c$^+$ macrophages in the inflammation prone VAD (Fig. 1g), but not the subcutaneous adipose (SAD), excluding a general defect in macrophage recruitment. Reduced VAD macrophage numbers likely reflected improved obesity in the protected strains.

TF-PAR2 signaling promotes macrophage inflammation

Monocyte/macrophage TF is induced by NFκB and JNK signaling pathways[27] that are crucial for the development of proinflammatory adipose tissue macrophages[24]. TF was expressed by CD11b$^+$/F4/80$^+$ macrophages specifically in the inflammation prone VAD and at higher levels in CD11b$^+$/CD11c$^+$ versus CD11b$^+$/CD11c$^-$ adipose tissue macrophages (Fig. 2a). To determine the contributions of macrophage TF-PAR2 signaling to adipose inflammation, we reconstituted lethally irradiated WT type mice with bone marrow (BM) from TF$^{\Delta CT}$ or *F2rl1*$^{-/-}$ mice. After 6 weeks of engraftment, we fed mice a HFD for 16 to 19 weeks. Deletion of the TF cytoplasmic domain or PAR2 in the hematopoietic compartment did not impair HFD-induced weight gain (Fig. 2b), suggesting that TF-PAR2 signaling in non-hematopoietic cells promoted obesity.

Donor BM-derived cells accounted for >90% of the VAD macrophages (Fig. 2c) and TF expression in VAD CD11b$^+$/CD11c$^+$ adipose tissue macrophages was indistinguishable between mice reconstituted with knock-out or WT BM (Supplementary Fig. 3). However, TF$^{\Delta CT}$ and *F2rl1*$^{-/-}$ BM chimeras had reduced numbers of VAD CD11b$^+$/CD11c$^+$ macrophages, but no appreciable changes in CD11b$^+$/CD11c$^-$ macrophages or CD4$^+$ or CD8$^+$ T cell numbers (Fig. 2d). Despite the normal HFD-induced weight gain, chimeras deficient in hematopoietic TF-PAR2 signaling showed reduced blood glucose levels and improved glucose tolerance and insulin sensitivity relative to WT controls (Fig. 2c; Supplementary Fig. 4). Adipose tissues of these chimeric mice had lower mRNA levels of the pro-inflammatory cytokine IL-6 and increased levels of the anti-inflammatory cytokine IL-10 (Fig. 2e).

TF regulates reverse endothelial transmigration contributing to dendritic cell maturation[28] that may cause reduced CD11b$^+$/11c$^+$ macrophage recruitment. However, TF cytoplasmic domain signaling also regulates activation of myeloid cells[21, 29] and, in microglia, PAR2 triggers induction of TNFα and IL-6, while PAR2-deficiency results in increased IL-10 expression[30]. In an independent experiment, cytokine mRNA expression in isolated CD11b$^+$ macrophages showed a reduction in IL-6 and increased IL-10 in TF-PAR2 signaling-deficient macrophages (Fig. 2e). Thus, hematopoietic TF-PAR2 signaling plays no role in

the development of obesity, but promotes HFD-induced adipose tissue macrophage inflammation and insulin resistance.

Macrophage inflammation also contributes to hepatic steatosis[5, 31] confirmed by histological and biochemical analysis to be reduced in the BM TF-PAR2 signaling-deficient chimeric mice (Fig. 2f). However, skeletal muscle triglyceride concentrations were modestly increased compared to WT chimeras (Fig. 2f, 2g), consistent with other models where reduced myeloid cell inflammation is associated with reduced steatosis, modest increases in muscle triglycerides and improved insulin sensitivity[32]. Accumulation of triglycerides in muscle can improve insulin sensitivity by sequestering reactive lipid metabolites such as ceramide that causes insulin resistance[33, 34]. Thus, improvements in adipose, hepatic and muscle insulin sensitivity likely contributed to improved glucose homeostasis in inflammation-protected $TF^{\Delta CT}$ or *F2rl1*$^{-/-}$ BM chimeric mice.

Inhibition of TF signaling improves insulin sensitivity

$TF^{\Delta CT}$ and *F2rl1*$^{-/-}$ adipose tissue macrophages appeared indistinguishable from WT in the expression of CD11b/CD11c surface markers, but it remained unproven that TF-PAR2 signaling directly sustained their pro-inflammatory phenotype. We used knock-in mice carrying human TF under control of the endogenous TF promoter (TFKI mice)[35] to generate BM chimeras in which hematopoietic cells were humanized for TF. On a HFD, these chimeric mice developed obesity and insulin resistance indistinguishable from WT BM controls (Supplementary Fig. 5a, b). In these chimeric mice, human TF is only expressed in BM-derived myeloid cells allowing us to selectively block macrophage TF with the species-selective monoclonal antibody 10H10 to human TF that inhibits TF-VIIa-PAR2 signaling, but not coagulation[21, 23].

A single dose of monoclonal antibody 10H10 within 24 hours significantly decreased basal blood glucose (214±15 versus 245±18 mg/dL; $p<0.05$) and improved glucose homeostasis in the TFKI BM chimeras relative to chimeric mice treated with isotype-matched control antibody or wild-type BM chimera controls receiving 10H10 (Fig. 3a). Specific antibody treatment decreased mRNA levels of pro-inflammatory cytokines TNF-α and IL-6 and increased mRNA levels of the anti-inflammatory IL-10 in VAD $CD11b^+$ macrophages, but PAI-1 mRNA levels were unchanged demonstrating specificity (Fig. 3b). Notably, treatment of obese BM TFKI mice with antibody to human TF did not appreciably reduce VAD $CD11b^+/CD11c^+$ macrophage counts relative to control antibody (Fig. 3b), excluding that the antibody to TF caused macrophage depletion. Since BM transplantation replaces myeloid cells in the liver[31, 36], it is likely that TF blockade also improved hepatic inflammation to improve overall insulin sensitivity.

In an independent approach, we acutely blocked TF in obese wild-type mice with monoclonal antibody 21E10 that inhibits binding of VIIa to murine TF. This treatment also improved glucose tolerance within 24 hours (Fig. 3c) and was specific, since this antibody specific for mouse TF did not further improve insulin resistance of insulin-sensitive HFD $TF^{\Delta CT}$ mice relative to control antibody (Supplementary Fig. 5c). As seen with selective TF blockade of myeloid cells, antibody 21E10-treated obese WT mice showed decreased VAD mRNA levels of TNF-α and IL-6, increased IL-10, and unchanged counts of $CD11b^+$/

CD11c$^+$ macrophages relative to control antibody (Fig. 3d). Analysis of isolated adipose CD11b$^+$ macrophages (Fig. 3e) confirmed these cytokine changes (Fig. 3e). However, total blockade of TF reduced mRNA levels of PAI-1 in VAD but not in isolated macrophages, indicating that TF-PAR2 signaling also occurred in a non-hematopoietic cell type, presumably the adipocyte. Thus, inhibition of TF signaling rapidly changes adipose tissue macrophage phenotypes to improve insulin sensitivity in obesity.

TF-PAR2 signaling in non-hematopoietic cells promotes obesity

To address roles of non-hematopoietic TF-PAR2 signaling in the development of obesity, we transplanted WT BM into TF$^{\Delta CT}$ and *F2rl1*$^{-/-}$ mice. Compared to WT recipient controls, mice with a TF-PAR2 signaling-deficient stromal compartment showed reduced HFD-induced weight gain (Fig. 4a). Histological analysis of 18 weeks HFD mice showed reduced abundance of CLS in VAD, reduced liver weight, hepatic steatosis, and muscle triglyceride accumulation in chimeric TF$^{\Delta CT}$ and *F2rl1*$^{-/-}$ mice compared to WT controls (Fig. 4b, c). The metabolically favorable changes were reflected in reduced FFA and blood glucose in chimeric mutants (Fig. 4c). FACS analysis of VAD SVF cells confirmed reduced CD11b$^+$/CD11c$^+$ macrophage numbers, indicating that improvements in obesity indirectly caused reduced recruitment of macrophages with normal TF-PAR2 signaling (Fig. 4c).

WT BM chimeric TF$^{\Delta CT}$ and *F2rl1*$^{-/-}$ were hyperphagic and more active than WT recipient controls, excluding that the reduced weight gain was caused by decreased food intake (Fig. 4d). Both TF$^{\Delta CT}$ mice with WT BM (Fig. 4d) and whole body TF$^{\Delta CT}$ mice (Supplementary Fig. 6a) showed increased oxygen consumption and CO_2 output in indirect calorimetry, with unchanged or slightly decreased respiratory exchange ratios (RER) relative to WT controls, suggesting that increased metabolism in the absence of major impairments of fat utilization contributed to the reduced body weight in TF$^{\Delta CT}$ mice. To eliminate differences in body weight and activity as variables, we further blocked TF acutely in obese WT mice during metabolic evaluation. Blocking TF with the antibody 21E10 in weight-matched DIO mice caused no changes in activity or food intake relative to control antibody, but significantly increased oxygen consumption and CO_2 output with a modest reduction of the RER indicative of improved fatty acid oxidation (Fig. 4e). Since TF is not detectable in skeletal muscle cells or hepatocytes by in situ hybridization[37, 38], the improved energy expenditure and metabolism following anti-TF therapy or genetic TF cytoplasmic domain deletion in the stromal compartment likely originated from alteration of TF signaling in the adipocyte.

Despite increased food intake and activity, oxygen consumption and CO_2 output were not significantly increased in WT BM chimeric *F2rl1*$^{-/-}$ mice relative to WT controls (Fig. 4d). Similarly, metabolism was not increased in an experiment with whole body *F2rl1*$^{-/-}$-deficient mice displaying no increased activity and food intake (Supplementary Fig. 6b). However, VO_2 and CO_2 were significantly increased for *F2rl1*$^{-/-}$ groups when normalized for body weights (Supplementary Fig. 6c, d). A modest, but significant increase of RER of *F2rl1*$^{-/-}$ mice relative to WT indicated impaired fatty acid oxidation, consistent with the proposed role of adipocyte PAR2 G protein-coupled signaling in activating AMPK[12]. However, similar to TF$^{\Delta CT}$ chimeric mice, WT BM *F2rl1*$^{-/-}$ mice had reduced TG levels in

liver and skeletal muscle (Fig. 4b, c), indicating that deletion of TF or PAR2 signaling in adipocytes has common beneficial effects on other insulin-sensitive tissues.

Adipocyte TF-VIIa signaling controls regulators of obesity

Considering that PAR2 β-arrestin signaling suppresses PI-3 kinase activation and that insulin-induced Akt phosphorylation was not inhibited in obese $TF^{\Delta CT}$ mice (Fig. 1), we asked whether adipocyte Akt activation was directly regulated by TF-VIIa-PAR2 signaling. In *in vitro* differentiated adipocytes from WT, but not from $TF^{\Delta CT}$ mice, VIIa suppressed basal Akt phosphorylation in a TF-dependent manner (Fig. 5a). Insulin-induced Akt phosphorylation was similarly inhibited in VIIa-treated WT, but not in $TF^{\Delta CT}$ adipocytes (Fig. 5b). Importantly, Akt activation was preserved in insulin-treated WT adipocytes when VIIa binding to TF was blocked with antibody 21E10 to mouse TF. Thus, TF directly regulates adipocyte Akt activation.

Adipocyte TF-VIIa signaling regulated Akt-dependent target genes implicated in obesity and insulin resistance (Fig. 5c). Stimulation of 3T3-L1 adipocytes for 3 hours with VIIa, but not thrombin (not shown), increased in a TF-dependent manner mRNA expression of the obesity promoter PAI-1 that is negatively regulated by Akt in adipocytes[39]. Akt activation supports adiponectin expression in adipocytes[40]. VIIa stimulation reduced mRNA of this adipokine that upregulates glucose and lipid metabolism broadly in other insulin-sensitive tissue and thereby prevents obesity[414243]. Adiponectin activates AMPK and, consistently, VIIa suppressed the mRNA expression of targets downstream of AMPK, i.e. UCP-2 and PPAR-α involved in energy expenditure[44] and fatty acid oxidation[45]. Suppression of AMPK may, in part, also be directly mediated by β-arrestin downstream of TF-VIIa-PAR2 signaling[12]. In addition, TF-VIIa signaling increased adipocyte mRNA synthesis of TNF-α, a key inflammatory mediator that promotes obesity and insulin resistance[46]. Thus, adipocyte TF-VIIa signaling regulates crucial effectors that contribute to the development of DIO.

To demonstrate that TF signaling *in vivo* regulated the same target genes, adipocytes were isolated from the VAD of WT mice 24 hours after treatment with antibody 21E10 to mouse TF. Blockade of TF reduced mRNA levels of PAI-1 and TNF-α and increased mRNA expression of adiponectin, UCP-2 and PPAR-α (Fig. 5d), demonstrating a reversal of TF-VIIa signaling effects observed in cultured adipocytes. These changes were directly caused by TF adipocyte signaling, because the mouse TF-specific antibody 21E10 (Supplementary Fig. 7) caused the same changes in treated BM chimeric mice with human TF in hematopoietic cells (Fig. 5d). Conversely, blocking human TF signaling in the hematopoietic compartment of the chimeric mice with antibody 10H10 had no effect on the adipocyte expression of the same target genes relative to control. These data establish direct and independent regulatory roles for adipocyte TF signaling in the expression of key mediators of weight gain[42, 47–49].

TF is expressed by neither skeletal muscle nor hepatocytes[3738] and restrictions of the blood-brain barrier would exclude central effects of acutely administered antibody. Blocking adipocyte TF in the human/mouse TF chimeric mice ameliorated insulin resistance within 24 hours (Fig. 5e). In order to determine whether the improved insulin sensitivity was independent of changes in adipose inflammation, we determined inflammatory cytokines in

SVF cells which include macrophages (Fig. 5f). As expected, blocking hematopoietic TF signaling with the human TF-specific antibody 10H10 increased IL-10 and suppressed IL-6 and TNF-α mRNA levels in SVF cells from these chimeric mice. Blocking TF specifically in non-hematopoietic cells with the murine TF-specific antibody 21E10 had no effect on IL-10 mRNA expression. Thus, macrophage TF signaling specifically regulates IL-10 expression independent of potential cross talks from adipocytes. Conversely, both antibodies did not change PAI-1 mRNA expression in SVF cells, confirming adipocyte-specific regulation of PAI-1 by TF signaling. However, inhibition of non-hematopoietic TF reduced mRNA levels of TNF-α and IL-6 in SVF cells. These data indicated that improved insulin sensitivity in response to TF blockade on adipocytes may, in part, involve reduced adipose tissue inflammation.

Discussion

This study establishes an unexpected direct role for coagulation signaling in the development of obesity and insulin resistance. Consistent with established pro-inflammatory effects of TF cytoplasmic domain and PAR2 signaling in myeloid cells[21, 29], genetic loss of this signaling pathway attenuates adipose macrophage inflammation and improves insulin sensitivity. Significantly, acute blockade of macrophage TF-VIIa signaling produces a rapid phenotypic switch of adipose tissue pro-inflammatory macrophages, decreasing the expression of TNF-α and IL-6, and increasing levels of the anti-inflammatory cytokine IL-10 (Supplementary Fig. 8). These changes in macrophage phenotype are directly linked to insulin sensitivity, since neutralization of TNF-α enhances insulin signaling in the adipose tissue and muscle[46, 50, 51], reduction of adipose IL-6 improves hepatic insulin resistance by down regulation of SOCS3[52], and IL-10 protects against TNF-α-mediated insulin resistance in adipocytes[53]. Importantly, selective blockade of macrophage TF signaling in chimeric mice was sufficient to reverse insulin resistance independent of changes in adipocyte-derived metabolic regulators. The phenotypic switch of adipose tissue macrophage in these mice was reminiscent of the macrophage-mediated anti-inflammatory and insulin sensitizing effects following activation of GPR120 by omega-3 fatty acid[2].

While our data show that TF signaling is a direct regulator of adipose tissue macrophage inflammation, TF in the non-hematopoietic compartment induced adipocyte expression of PAI-1 and indirectly supported macrophage production of TNF-α and IL-6, but not IL-10. The reduction of macrophage inflammatory cytokines was observed in mice treated with the antibody 21E10 that reversed PAI-1 expression in adipocytes and also directly blocked coagulation. This suggests the intriguing possibility that adipocyte TF-induced coagulation in conjunction with PAI-1-mediated suppression of fibrinolysis may increase local fibrin deposition required for the proinflammatory phenotype of adipose tissue macrophages. Indeed, integrin $\alpha_M\beta_2$ interaction with fibrin is crucial for macrophage activation and inflammatory cytokine production[54–56]. Thus, the mechanistic coupling of fibrin generation and innate immune cell-driven inflammation may cause adipose tissue inflammation and metabolic syndrome.

Absence of TF cytoplasmic domain signaling in non-hematopoietic cells produced an obesity resistant phenotype. Acute disruption of the ligand interaction between TF and VIIa

rapidly improved metabolism independent of changes in body weight, food intake, or locomotor activity. Mechanistically, adipocyte TF-VIIa signaling initiates a TF cytoplasmic domain-dependent suppression of basal and insulin-mediated Akt phosphorylation and alters the expression of Akt-regulated target genes causally linked to weight gain in DIO[14, 42, 45, 48, 49]. Of these, adiponectin, an adipokine produced exclusively by adipocytes regulates glucose uptake, AMPK activation and fatty acid oxidation, and has additional central effects on body weight reduction[42]. Thus, TF-Vlla-mediated suppression of adipocyte adiponectin broadly influences insulin responsive target tissue, reduces energy expenditure, and thereby contributes to an obese phenotype (Supplementary Fig. 8). Importantly, these experiments demonstrate synergistic and independent roles for adipocyte and immune cell TF signaling in the metabolic impairments of obesity.

Improving insulin resistance without the side effects of weight gain, as is observed for PPARγ agonists remains a major challenge for anti-diabetic therapies. A rapidly acting signaling blocking anti-TF antibody with minimal risks of bleeding complications may provide a novel approach to target the metabolic complications of obesity and potentially induce weight loss by independent effects on the regulation of energy expenditure by adipocytes.

Methods

Animals

All experiments were approved by the animal ethics committee of the Torrey Pines Institute for Molecular Studies and The Scripps Research Institute IACUC. We backcrossed $TF^{\Delta CT}$ [57], *F2rl1*$^{-/-}$ [58], and $TF^{\Delta CT}$/*F2rl1*$^{-/-}$ mice for at least 9 generations into C57BL/6J. Humanized TF knock-in mice (TFKI) in the C57BL/6J background[21] were originally developed by Lexicon Pharmaceuticals. We fed male mice a HFD (60% kcal from fat; Research Diets) beginning at 6–8 weeks of age. We generated BM chimeras by injecting 5–10 × 10^6 BM cells 4–6 hours after lethal irradiation of mice and started mice on a HFD for 16–20 weeks following engraftment under antibiotic prophylaxis for 6 weeks. BM donors typically carried a transgene for green fluorescent protein (GFP) (C57BL/6-Tg(CAG-EGFP)131Osb/LeySopJ; Jackson) and we quantified reconstitution efficiency of adipose tissue macrophages by determining GFP-positivity of $CD11b^+$/$CD11c^+$ cells, using gates established by GFP^{neg} control SVF cells prepared identically.

Indirect Calorimetry

We evaluated metabolism of mice placed in respiratory chambers equipped with a food tray connected to a balance and photo beams to detect motor activity (Oxymax, Columbus Instruments) under the regular 12 hour light-dark cycle[59]. We measured oxygen consumption (VO_2) and CO_2 production (VCO_2) from each metabolic chamber every 15 min for 3 consecutive days and averaged data based on light-dark cycles.

Glucose and Insulin challenge

We injected mice fasted for 6 hours intraperitoneally with glucose (2 g per kilogram body weight) or non-fasted mice with insulin (0.75U/kg, Eli Lilly) and determined glucose

concentration with a Glucometer (Bayer) in blood samples from tail bleeds at baseline and 15, 30, 60, 90 and 120 minutes after injection. For insulin-dependent Akt phosphorylation, we injected mice with 0.75U/kg insulin via the tail vein 10 minuted prior to harvesting VAD samples for Western blotting using antibodies (Cell Signaling Technology) for phosphorylated Akt serine 473 of Akt[59].

Adipocyte culture

We differentiated 3T3-L1 mouse embryo fibroblasts or adipose SVF into adipocytes[60] and incubated the cells in serum free media 24 hours prior to treatment with VIIa (25 nM) in the presence or absence of 50 μg/ml antibody 21E10 to mouse TF. After 3 hours we extracted total RNA and measured gene expression. We treated differentiated adipocytes with VIIa in serum free media for 24 hours and stimulated with 100 nM insulin for 10 minutes for analysis of Akt serine 473 phosphorylation by Western blotting[59].

Analysis of gene expression

We extracted total RNA with the Ultraspec RNA isolation system (Biotecx Laboratories, Houston, TX), synthesized cDNA and performed real-time quantitative RT-PCR with gene-specific primers (Invitrogen) and SYBR Green PCR Master mix (PerkinElmer) in an iCycler (Bio-Rad)[59]. Relative gene expression levels were calculated after normalization to β-actin using the $\Delta\Delta C_T$ method (Bio-Rad).

Tissue factor assay

We used the TF activity kit (American Diagnostica) to measure TF activity in plasma and adipose tissues extracts obtained by homogenization in 15 mM octyl-β-D-glucopyranoside, 25 mM HEPES-buffered normal saline (pH 7.0) followed by recovery of supernatants after centrifugation at 15,600 g for 5 min.

Adipose tissue fractionation

We washed and minced epididymal adipose tissues in PBS containing 0.5% BSA, performed initial clearance by centrifugation for 5 min at 1680 rpm, or directly incubated tissues at 37°C on a shaking platform for 20 min with collagenase (1 mg/ml) in the same buffer. We filtered the suspension through a nylon filter (100 μm), centrifuged for 5 min at 1680 rpm at 4°C, and recovered the floating cells and the pellet as the mature adipocytes and the stromal vascular fraction (SVF), respectively.

Flow cytometry and CD11b$^+$ selection

We stained SVF cells following incubation for 5 min in RBC lysis buffer in FACS buffer (PBS, 1% FCS, 1 mM EDTA) at 4°C for 30 min with labeled monoclonal antibodies to CD3, CD4, CD8α, CD11b, CD11c, F4/80 (eBioscience), or TF (PhD126) in the presence of Fc receptor blocking antibody CD16/32 (eBioscience). We employed propidium iodide (PI, Invitrogen) for live cell gating and fixed washed cells with 1% formaldehyde for analysis on a LSR-II cytometer (BD) with data processing using the FlowJo software (Tree Star). SVF from 2–3 mice were typically pooled. We selected CD11b$^+$ cells from SVF using anti-

CD11b paramagnetic microbeads (Milltenyi) by a single pass through the magnetic columns.

Tissue triglyceride quantification

We homogenized liver and muscle samples (20–30mg) for 10 min in 1 ml of isopropanol using a Pro200 homogenizer, centrifuged (2000 g for 10 min) to recover 100μl of supernatant for drying in a Speedvac system. We dissolved the dry residue in isopropanol for determination of triglyceride content with a Triglyceride E test (Wako).

Statistical analysis

We determined statistical significance of differences between two groups by unpaired Student's t-test and comparisons among several groups by ANOVA followed by the Bonferroni test.

Supplementary Material

Refer to Web version on PubMed Central for supplementary material.

Acknowledgements

This study was supported by US National Institutes of Health grants HL71146, HL104232 (F. Samad), HL77753 (W. Ruf), a grant from the Diabetes National Research Group (F. Samad), and a postdoctoral fellowship from the American Heart Association (C. Furlan-Freguia). We thank M. Anderson (J&J PRD) for TFKI mice, C. Biazak, J. Royce, N. Vu, and R. Zubairi for technical assistance, A. J. Roberts for assistance with the metabolic studies, and C. Johnson for preparation of figures.

References

1. Kadowaki T, et al. Adiponectin and adiponectin receptors in insulin resistance, diabetes, and the metabolic syndrome. J Clin Invest. 2006; 116:1784–1792. [PubMed: 16823476]
2. Oh DY, et al. GPR120 is an omega-3 fatty acid receptor mediating potent anti-inflammatory and insulin-sensitizing effects. Cell. 2010; 142:687–698. [PubMed: 20813258]
3. Nishimura S, et al. CD8+ effector T cells contribute to macrophage recruitment and adipose tissue inflammation in obesity. Nat Med. 2009; 15:914–920. [PubMed: 19633658]
4. Feuerer M, et al. Lean, but not obese, fat is enriched for a unique population of regulatory T cells that affect metabolic parameters. Nat Med. 2009; 15:930–939. [PubMed: 19633656]
5. Ouchi N, et al. Sfrp5 is an anti-inflammatory adipokine that modulates metabolic dysfunction in obesity. Science. 2010; 329:454–457. [PubMed: 20558665]
6. Odegaard JI, et al. Macrophage-specific PPARgamma controls alternative activation and improves insulin resistance. Nature. 2007; 447:1116–1120. [PubMed: 17515919]
7. Rajagopal S, Rajagopal K, Lefkowitz RJ. Teaching old receptors new tricks: biasing seven-transmembrane receptors. Nat Rev Drug Discov. 2010; 9:373–386. [PubMed: 20431569]
8. Wang P, DeFea KA. Protease-activated receptor-2 simultaneously directs beta-arrestin-1-dependent inhibition and Galphaq-dependent activation of phosphatidylinositol 3-kinase. Biochemistry. 2006; 45:9374–9385. [PubMed: 16878972]
9. Luan B, et al. Deficiency of a beta-arrestin-2 signal complex contributes to insulin resistance. Nature. 2009; 457:1146–1149. [PubMed: 19122674]
10. Wang P, Kumar P, Wang C, DeFea KA. Differential regulation of class IA phosphoinositide 3-kinase catalytic subunits p110 alpha and beta by protease-activated receptor 2 and beta-arrestins. Biochem J. 2007; 408:221–230. [PubMed: 17680774]

11. Zoudilova M, et al. Beta-arrestin-dependent regulation of the cofilin pathway downstream of protease-activated receptor-2. J Biol Chem. 2007; 282:20634–20646. [PubMed: 17500066]
12. Wang P, Jiang Y, Wang Y, Shyy JY, DeFea KA. Beta-arrestin inhibits CAMKKbeta-dependent AMPK activation downstream of protease-activated-receptor-2. BMC Biochem. 2010; 11:36. [PubMed: 20858278]
13. Hotamisligil GS. Inflammation and metabolic disorders. Nature. 2006; 444:860–867. [PubMed: 17167474]
14. De TB, Smith LH, Vaughan DE. Plasminogen activator inhibitor-1: a common denominator in obesity, diabetes and cardiovascular disease. Curr Opin Pharmacol. 2005; 5:149–154. [PubMed: 15780823]
15. Gerrits AJ, Koekman CA, VAN Haeften TW, Akkerman JW. Increased tissue factor expression in diabetes mellitus type 2 monocytes caused by insulin resistance. J Thromb Haemost. 2011; 9:873–875. [PubMed: 21251203]
16. Diamant M, et al. Elevated numbers of tissue-factor exposing microparticles correlate with components of the metabolic syndrome in uncomplicated type 2 diabetes mellitus. Circulation. 2002; 106:2442–2447. [PubMed: 12417540]
17. Kopp CW, et al. Weight loss reduces tissue factor in morbidly obese patients. Obes. Res. 2003; 11:950–956. [PubMed: 12917499]
18. Samad F, Pandey M, Loskutoff DJ. Tissue factor gene expression in the adipose tissues of obese mice. Proc. Natl. Acad. Sci. USA. 1998; 95:7591–7596. [PubMed: 9636194]
19. Dorfleutner A, Hintermann E, Tarui T, Takada Y, Ruf W. Cross-talk of integrin alpha3beta1 and tissue factor in cell migration. Mol Biol Cell. 2004; 15:4416–4425. [PubMed: 15254262]
20. Schaffner F, et al. Cooperation of Tissue Factor Cytoplasmic Domain and PAR2 Signaling in Breast Cancer Development. Blood. 2010; 116:6106–6113. [PubMed: 20861457]
21. Redecha P, Franzke CW, Ruf W, Mackman N, Girardi G. Neutrophil activation by the tissue factor/Factor VIIa/PAR2 axis mediates fetal death in a mouse model of antiphospholipid syndrome. J Clin Invest. 2008; 118:3453–3461. [PubMed: 18802482]
22. Ahamed J, et al. Disulfide isomerization switches tissue factor from coagulation to cell signaling. Proc Natl Acad Sci U S A. 2006; 103:13932–13937. [PubMed: 16959886]
23. Versteeg HH, et al. Inhibition of tissue factor signaling suppresses tumor growth. Blood. 2008; 111:190–199. [PubMed: 17901245]
24. Olefsky JM, Glass CK. Macrophages, inflammation, and insulin resistance. Annu Rev Physiol. 2010; 72:219–246. [PubMed: 20148674]
25. Patsouris D, et al. Ablation of CD11c-positive cells normalizes insulin sensitivity in obese insulin resistant animals. Cell Metab. 2008; 8:301–309. [PubMed: 18840360]
26. Cinti S, et al. Adipocyte death defines macrophage localization and function in adipose tissue of obese mice and humans. J Lipid Res. 2005; 46:2347–2355. [PubMed: 16150820]
27. Guha M, Mackman N. LPS induction of gene expression in human monocytes. Cell Signal. 2001; 13:85–94. [PubMed: 11257452]
28. Randolph GJ, Luther T, Albrecht S, Magdolen V, Muller WA. Role of tissue factor in adhesion of mononuclear phagocytes to and trafficking through endothelium in vitro. Blood. 1998; 92:4167–4177. [PubMed: 9834221]
29. Ahamed J, et al. Regulation of macrophage procoagulant responses by the tissue factor cytoplasmic domain in endotoxemia. Blood. 2007; 109:5251–5259. [PubMed: 17332247]
30. Noorbakhsh F, et al. Proteinase-activated receptor 2 modulates neuroinflammation in experimental autoimmune encephalomyelitis and multiple sclerosis. J Exp. Med. 2006; 203:425–435. [PubMed: 16476770]
31. Odegaard JI, et al. Alternative M2 activation of Kupffer cells by PPARdelta ameliorates obesity-induced insulin resistance. Cell Metab. 2008; 7:496–507. [PubMed: 18522831]
32. Saberi M, et al. Hematopoietic cell-specific deletion of toll-like receptor 4 ameliorates hepatic and adipose tissue insulin resistance in high-fat-fed mice. Cell Metab. 2009; 10:419–429. [PubMed: 19883619]

33. Liu L, et al. Upregulation of myocellular DGAT1 augments triglyceride synthesis in skeletal muscle and protects against fat-induced insulin resistance. J Clin Invest. 2007; 117:1679–1689. [PubMed: 17510710]
34. Pickersgill L, Litherland GJ, Greenberg AS, Walker M, Yeaman SJ. Key role for ceramides in mediating insulin resistance in human muscle cells. J Biol Chem. 2007; 282:12583–12589. [PubMed: 17337731]
35. Snyder LA, et al. Expression of human tissue factor under the control of the mouse tissue factor promoter mediates normal hemostasis in knock-in mice. J Thromb. Haemost. 2008; 6:306–314. [PubMed: 18005233]
36. Bradshaw G, et al. Facilitated replacement of Kupffer cells expressing a paraoxonase-1 transgene is essential for ameliorating atherosclerosis in mice. Proc Natl Acad Sci U S A. 2005; 102:11029–11034. [PubMed: 16043712]
37. Mackman N, Sawdey MS, Keeton MR, Loskutoff DJ. Murine tissue factor gene expression *in vivo*: tissue and cell specificity and regulation by lipopolysaccharide. Am. J. Pathol. 1993; 143:76–84. [PubMed: 8317556]
38. Samad F, Pandey M, Loskutoff DJ. Regulation of tissue factor gene expression in obesity. Blood. 2001; 98:3353–3358. [PubMed: 11719374]
39. Venugopal J, Hanashiro K, Yang ZZ, Nagamine Y. Identification and modulation of a caveolae-dependent signal pathway that regulates plasminogen activator inhibitor-1 in insulin-resistant adipocytes. Proc Natl Acad Sci U S A. 2004; 101:17120–17125. [PubMed: 15569940]
40. Kidani T, et al. Bisphenol A downregulates Akt signaling and inhibits adiponectin production and secretion in 3T3-L1 adipocytes. J Atheroscler. Thromb. 2010; 17:834–843. [PubMed: 20467186]
41. Matsuzawa Y. Adiponectin: a key player in obesity related disorders. Curr Pharm Des. 2010; 16:1896–1901. [PubMed: 20370675]
42. Qi Y, et al. Adiponectin acts in the brain to decrease body weight. Nat Med. 2004; 10:524–529. [PubMed: 15077108]
43. Yamauchi T, et al. Adiponectin stimulates glucose utilization and fatty-acid oxidation by activating AMP-activated protein kinase. Nat Med. 2002; 8:1288–1295. [PubMed: 12368907]
44. Jager S, Handschin C, St-Pierre J, Spiegelman BM. AMP-activated protein kinase (AMPK) action in skeletal muscle via direct phosphorylation of PGC-1alpha. Proc Natl Acad Sci U S A. 2007; 104:12017–12022. [PubMed: 17609368]
45. Lee Y, et al. PPAR alpha is necessary for the lipopenic action of hyperleptinemia on white adipose and liver tissue. Proc Natl Acad Sci U S A. 2002; 99:11848–11853. [PubMed: 12195019]
46. Uysal KT, Wiesbrock SM, Marino MW, Hotamisligil GS. Protection from obesity-induced insulin resistance in mice lacking TNF-α function. Nature. 1997; 389:610–614. [PubMed: 9335502]
47. Guerre-Millo M, et al. Peroxisome proliferator-activated receptor alpha activators improve insulin sensitivity and reduce adiposity. J Biol Chem. 2000; 275:16638–16642. [PubMed: 10828060]
48. Surwit RS, et al. Diet-induced changes in uncoupling proteins in obesity-prone and obesity-resistant strains of mice. Proc Natl Acad Sci U S A. 1998; 95:4061–4065. [PubMed: 9520493]
49. Fleury C, et al. Uncoupling protein-2: a novel gene linked to obesity and hyperinsulinemia. Nat. Genet. 1997; 15:269–272. [PubMed: 9054939]
50. Hotamisligil GS, Shargill NS, Spiegelman BM. Adipose expression of tumor necrosis factor-α: Direct role in obesity-linked insulin resistance. Science. 1993; 259:87–91. [PubMed: 7678183]
51. Hotamisligil GS, Budavari A, Murray D, Spiegelman BM. Reduced tyrosine kinase activity of the insulin receptor in obesity-diabetes. Central role of tumor necrosis factor-α. J. Clin. Invest. 1994; 94:1543–1549. [PubMed: 7523453]
52. Sabio G, et al. A stress signaling pathway in adipose tissue regulates hepatic insulin resistance. Science. 2008; 322:1539–1543. [PubMed: 19056984]
53. Lumeng CN, Bodzin JL, Saltiel AR. Obesity induces a phenotypic switch in adipose tissue macrophage polarization. J Clin Invest. 2007; 117:175–184. [PubMed: 17200717]
54. Steinbrecher KA, et al. Colitis-associated cancer is dependent on the interplay between the hemostatic and inflammatory systems and supported by integrin alpha(M)beta(2) engagement of fibrinogen. Cancer Res. 2010; 70:2634–2643. [PubMed: 20233870]

55. Smiley ST, King JA, Hancock WW. Fibrinogen stimulates macrophage chemokine secretion through toll-like receptor 4. J Immunol. 2001; 167:2887–2894. [PubMed: 11509636]

56. Flick MJ, et al. Leukocyte engagement of fibrin(ogen) via the integrin receptor alphaMbeta2/Mac-1 is critical for host inflammatory response in vivo. J Clin Invest. 2004; 113:1596–1606. [PubMed: 15173886]

57. Melis E, et al. Targeted deletion of the cytosolic domain of tissue factor in mice does not affect development. Biochem. Biophys. Res Commun. 2001; 286:580–586. [PubMed: 11511099]

58. Damiano BP, et al. Cardiovascular responses mediated by protease-activated receptor-2 (PAR-2) and thrombin receptor (PAR-1) are distinguished in mice deficient in PAR-2 or PAR-1. J Pharmacol Exp. Ther. 1999; 288:671–678. [PubMed: 9918574]

59. Yang G, et al. Central role of ceramide biosynthesis in body weight regulation, energy metabolism, and the metabolic syndrome. Am J Physiol Endocrinol. Metab. 2009; 297:E211–E224. [PubMed: 19435851]

60. Samad F, Yamamoto K, Loskutoff DJ. Distribution and regulation of plasminogen activator inhibitor-1 in murine adipose tissue in vivo. Induction by tumor necrosis factor-alpha and lipopolysaccharide. J Clin Invest. 1996; 97:37–46. [PubMed: 8550848]

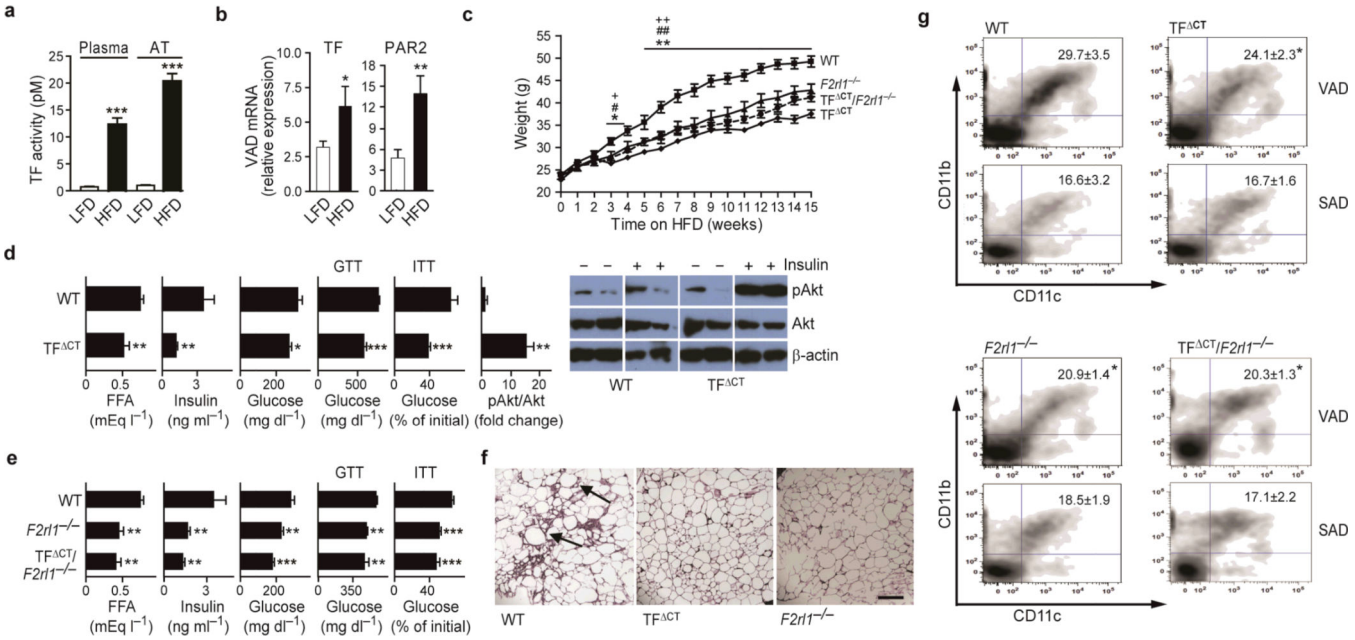

Fig. 1. TF-PAR2 signaling promotes diet induced obesity and insulin resistance

(**a**) TF activity in plasma and adipose tissue extracts of male C57BL/6J mice on low or high fat diet (LFD, 10% fat; HFD, 60% fat) for 16 weeks, $n = 6 \pm$ SD. (**b**) TF and PAR2 mRNA in VAD from 16 week HFD male C57BL/6J mice, $n = 6$, mean ± SD. For (**a–b**): $^{*}P < 0.05$, $^{**}P < 0.01$, $^{***}P < 0.001$ for LFD versus HFD. (**c**) HFD-induced weight gain of male $TF^{\Delta CT}$, *F2rl1*$^{-/-}$, $TF^{\Delta CT}$/*F2rl1*$^{-/-}$, or wild type (WT) mice; $n = 8–20$, mean ± SD. $^{*}P < 0.05$, $^{**}P < 0.01$, WT versus *F2rl1*$^{-/-}$; $^{\#}P < 0.05$, $^{\#\#}P < 0.01$ for WT versus $TF^{\Delta CT}$/*F2rl1*$^{-/-}$; $^{+}P < 0.05$, $^{++}P < 0.01$, for WT versus $TF^{\Delta CT}$. (**d**) Plasma levels, GTT, ITT, and insulin-mediated Akt phosphorylation in adipose tissues of HFD WT and $TF^{\Delta CT}$ mice. (**e**) Plasma levels, GTT and ITT for HFD WT, *F2rl1*$^{-/-}$ and $TF^{\Delta CT}$/*F2rl1*$^{-/-}$ mice. For (**d–e**): $n = 8–20$, mean ± SD. $^{*}P < 0.05$, $^{**}P < 0.01$, $^{***}P < 0.001$ for WT versus knock-out mice. (**f**) Representative H&E-stained, paraffin-embedded VAD sections from WT, $TF^{\Delta CT}$ and *F2rl1*$^{-/-}$ mice (n=3). Arrows indicate “crown like structures” of macrophages around apoptotic adipocytes. Scale bar: 50 μm. (**g**) FACS quantification of VAD and SAD $CD11b^{+}$/$CD11c^{+}$ macrophages in SVF from WT, $TF^{\Delta CT}$, *F2rl1*$^{-/-}$ and $TF^{\Delta CT}$/*F2rl1*$^{-/-}$ mice. SVF from 2–3 mice were typically pooled. $n = 3$, mean ± SD. $^{*}P < 0.05$ for WT versus knock-out mice.

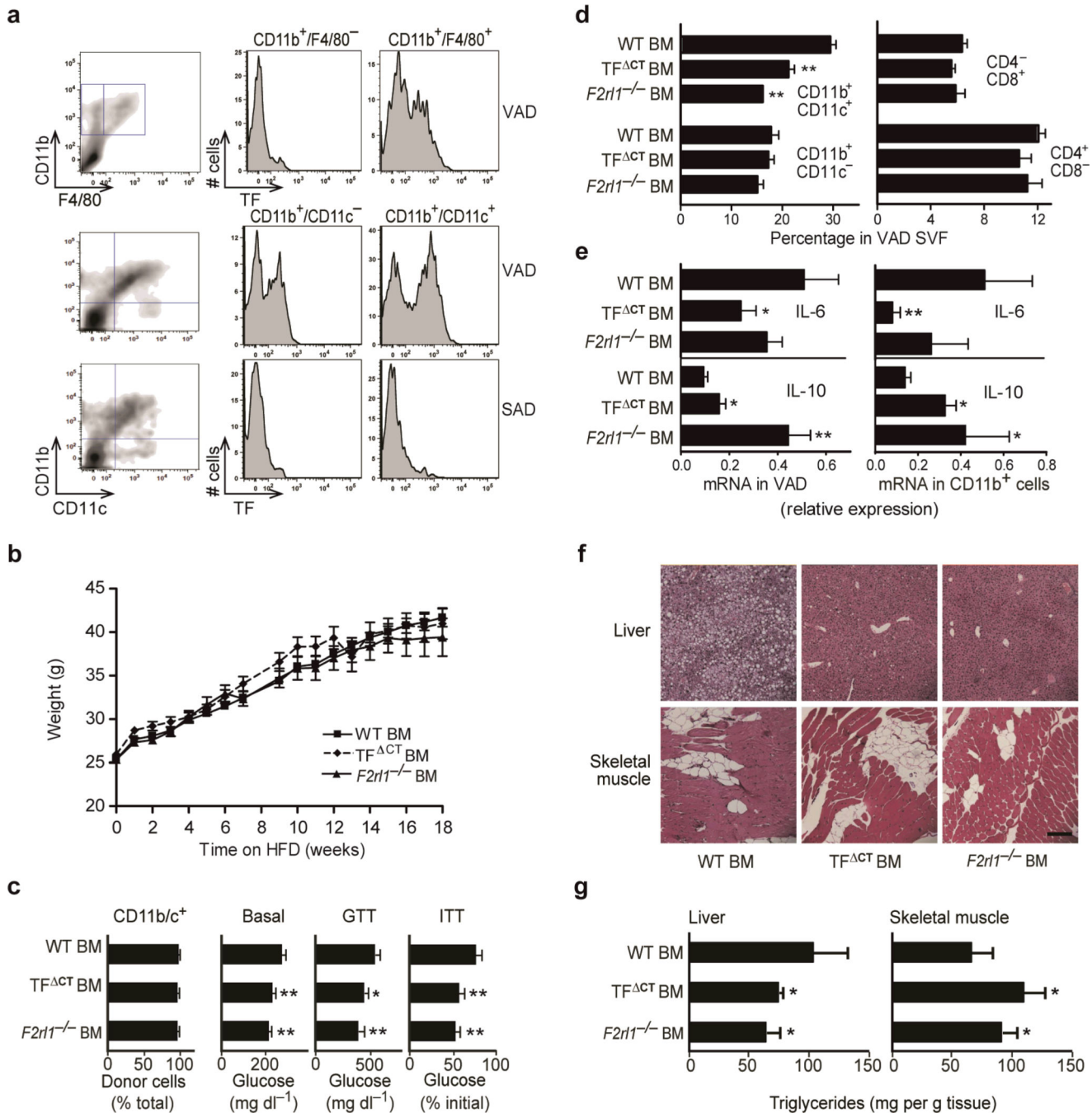

Fig. 2. TF-PAR2 signaling in hematopoietic cells contributes to insulin resistance and adipose tissue macrophage inflammation

(**a**) TF expression in $CD11b^+/F4/80+$ and $CD11b^+/F4/80^-$ or $CD11b^+/CD11c^-$ and $CD11b^+/CD11c^+$ gated macrophages in SVF from the VAD or SAD of WT DIO mice. (**b**) Weight gains of WT, $TF^{\Delta CT}$, or *F2rl1*$^{-/-}$ BM chimeras in C57BL/6 WT mice. Pooled data from 2 independent BM transplantation experiments, $n = 14$, mean ± SD. (**c**) Reconstitution efficiency of donor BM-derived macrophages labeled with green fluorescent protein (GFP). $n = 3$, mean ± SD. Plasma glucose, GTT, and ITT of $TF^{\Delta CT}$ or *F2rl1*$^{-/-}$ BM chimeras in

comparison with WT controls after 16 weeks of HFD. n = 10–14, mean ± SD. (**d**) FACS quantification of macrophage and T cell populations in the VAD SVF from WT, $TF^{\Delta CT}$, or $F2rl1^{-/-}$ BM chimeras. n = 3, mean ± SD. (**e**) IL-6 or IL-10 mRNA in VAD (n = 8, mean ± SD) or in CD11b-selected SFV cells (n = 4, mean ± SD) from WT, $TF^{\Delta CT}$, or $F2rl1^{-/-}$ BM chimeras. For (**c–e**): $*P < 0.05$, $**P < 0.01$ for WT versus the corresponding knock-out chimeras. (**f**) Representative H&E-stained paraffin-embedded sections of liver and muscle of chimeric mice with WT, $TF^{\Delta CT}$ and $F2rl1^{-/-}$ BM. Scale bar: 50 μm. (**g**) Triglyceride levels in liver and muscle of chimeric mice with WT, $TF^{\Delta CT}$ and $F2rl1^{-/-}$ BM after 16 weeks on the HFD. n = 12, mean ± SD; $*P < 0.05$ for WT versus knock-out chimeras.

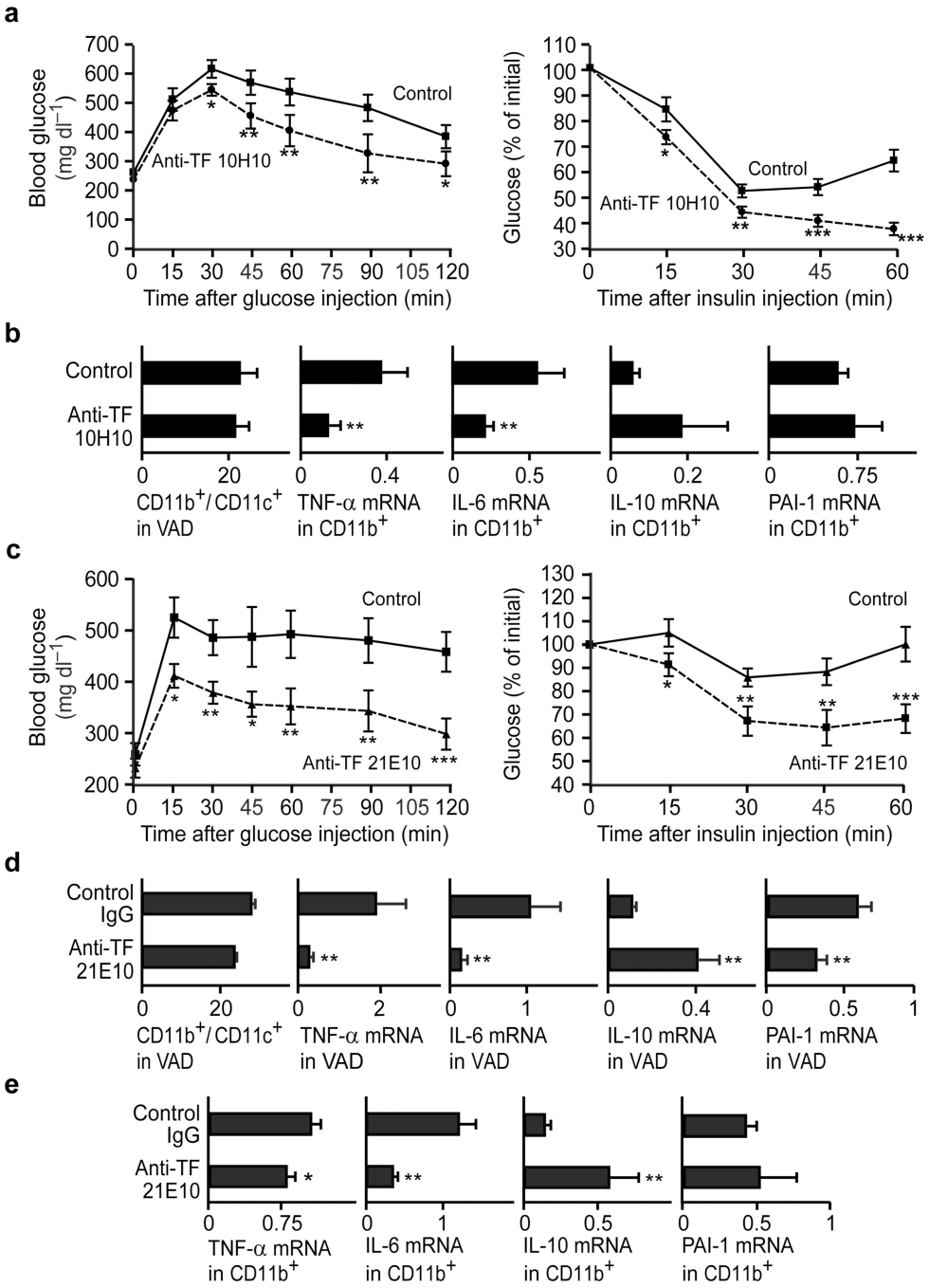

Fig. 3. Pharmacological inhibition of hematopoietic TF-PAR2 signaling ameliorates insulin resistance and adipose tissue macrophage inflammation

(**a**) GTT and ITT of obese TFKI BM chimeras 24 hours after receiving anti-human TF 10H10 (20 mg/kg) compared to either obese TFKI BM chimeras receiving non-specific IgG or control C57BL/6 WT BM chimeras receiving 10H10. The response of both control groups was indistinguishable and the data were combined to show a single control group. *n* = 4–8, mean ± SD; **P* < *0.05*, ***P* < *0.01* control versus antibody-treated. (**b**) $CD11b^+/CD11c^+$ macrophage counts in VAD and mRNA expression in VAD-derived $CD11b^+$-

selected macrophages 24 hours after treatment with 10H10. *n* = 3–6, mean ± SD; **P* < *0.05*, ***P* < *0.01* control versus antibody-treated. (**c**) Glucose and insulin tolerance test in 16 week HFD fed male WT obese mice 24 hours after intraperitoneal injection of rat anti-mouse TF 21E10 (20 mg/kg) or rat IgG control. *n* = 8, mean ± SD. (**d**) TNF-α, IL-6, IL-10 and PAI-1 mRNA, and $CD11b^+/CD11c^+$ macrophage counts in the VAD 24 hours after treatment with antibody 21E10 or control IgG. For gene expressions, *n* = 8, mean ± SD. For $CD11b^+/CD11c^+$ macrophages, n = 3 (pools of 2–3 mice). (**e**) mRNA expression in $CD11b^+$-selected VAD macrophages 24 hours after treatment with 21E10 or control IgG; *n* = 3–6, mean ± SD. For (**c–e**): **P* < *0.05*, ***P* < *0.01*, ****P* < *0.001* control versus specific antibody-treated.

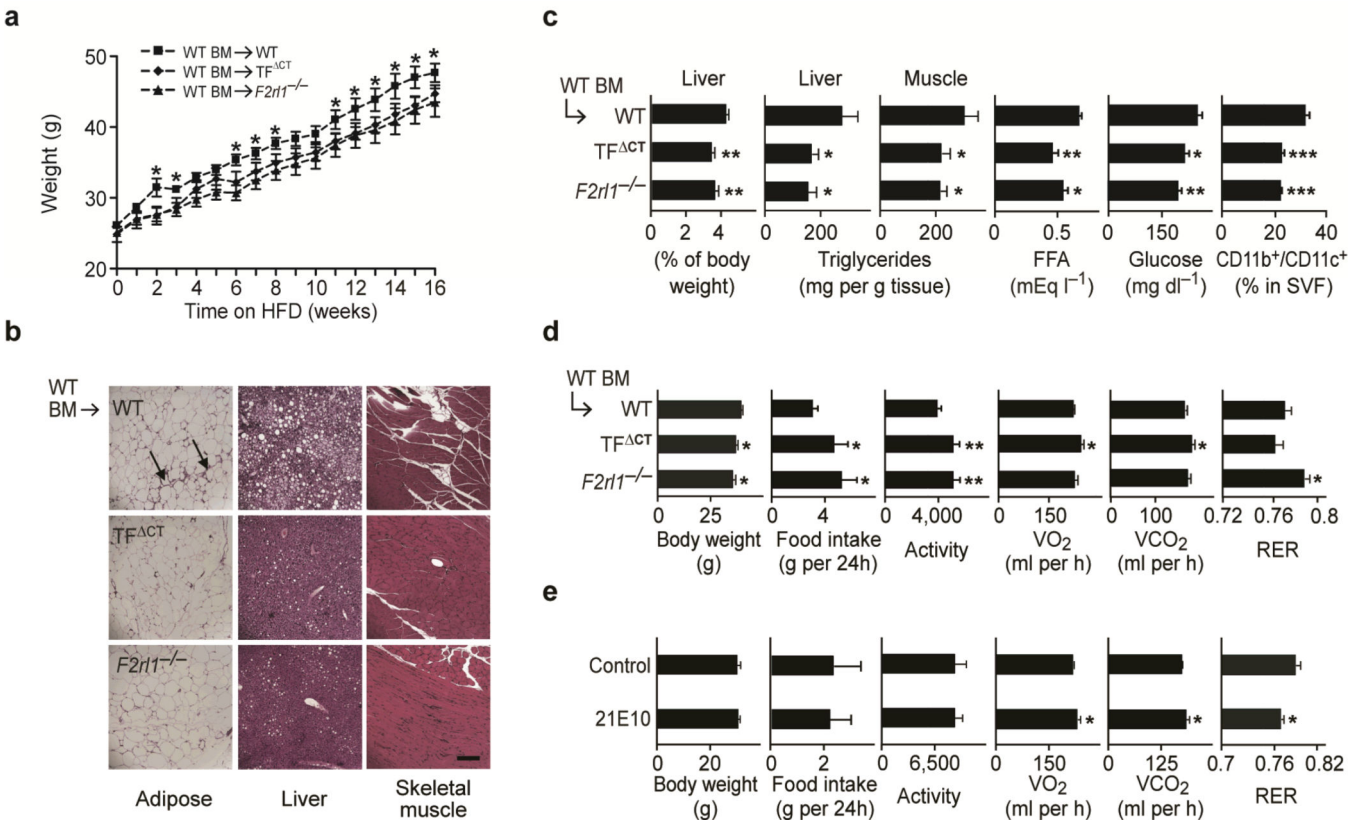

Fig. 4. TF-PAR2 signaling in non-hematopoietic cells contributes to DIO

(**a**) Weight gain of WT BM chimeras in WT, $TF^{\Delta CT}$ or *F2rl1*$^{-/-}$ mice on a HFD with confirmed >90% VAD reconstitution with GFP^+ donor macrophages. *n* = 8, mean ± SD. (**b**) Representative H&E-stained paraffin-embedded sections of VAD, liver and muscle of WT BM chimeric WT, $TF^{\Delta CT}$ and *F2rl1*$^{-/-}$ mice (*n* = 3). Scale bar: 50 μm, arrows indicate "crown like structures". (**c**) Liver weights, liver and muscle triglycerides, plasma FFA, glucose (*n* = 8, mean ± SD) and CD11b+/CD11c+ macrophages in VAD (*n* = 3) from HFD fed WT BM chimeras in WT, $TF^{\Delta CT}$ or *F2rl1*$^{-/-}$ mice. (**d**) Body weights, food intake, activity, oxygen consumption, $C0_2$ output and RER in BM chimeric mice (*n* = 5, mean ± SD). For (**a–d**): **P* < *0.05*, ***P* < *0.01*, ****P*<*0.001* for WT versus knock-out BM chimeras. (**e**) Body weights, food intake, activity and oxygen consumption, $C0_2$ output and RER in DIO mice following treatment with the anti-mouse TF antibody 21E10 (*n* = 5, mean ± SD). **P* < *0.05* for control versus 21E10 treated mice.

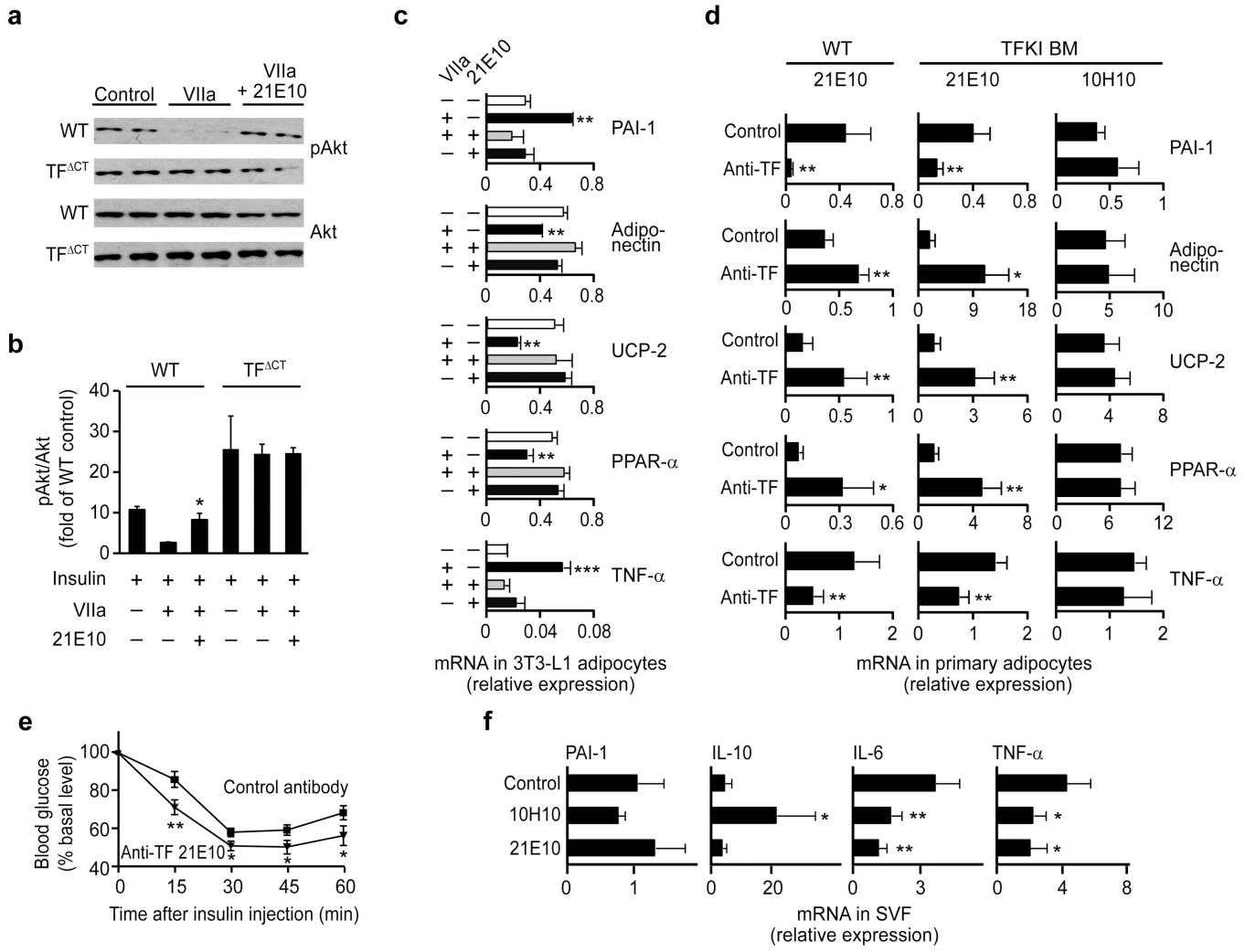

Fig. 5. Contributions of adipocyte TF-PAR2 signaling to the regulation of glucose and lipid metabolism in obesity

(**a**) Representative Western blot analysis for pAkt and Akt from control, VIIa, or VIIa + 21E10 treated primary adipocyte cultures from WT or $TF^{\Delta CT}$ mice. (**b**) Quantification of insulin-induced Akt phosphorylation after 24 hour treatment with or without VIIa of primary adipocyte cultures from WT and $TF^{\Delta CT}$ mice. n = 4–8, mean ± SD. (**c**) Regulation of gene expression in 3T3-L1 adipocytes by VIIa. n = 6, mean ± SD, $^{**}P < 0.01$, $^{***}P < 0.001$ for control versus VIIa-treated. (**d**) Gene expression in adipocytes isolated from VAD of DIO WT or TFKI BM chimeric mice treated overnight with antibody 21E10 to mouse TF or antibody 10H10 to human TF; n = 8–14, mean ± SD, $^{*}P < 0.05$, $^{**}P < 0.01$ for control versus antibody treated. (**e**) Insulin tolerance tests of obese TFKI BM chimeras 24 hours after receiving antibody 21E10 compared to obese TFKI BM chimeras receiving control IgG. (**f**) Gene expression in SVF fraction cells isolated from VAD of DIO TFKI BM chimeric mice treated with the murine TF specific antibody 21E10. For (**e, f**) n = 8, mean ± SD, $^{*}P < 0.05$, $^{**}P < 0.01$ for control versus antibody-treated.